Circulation

ORIGINAL RESEARCH ARTICLE

Low-Density Lipoprotein-Reactive T Cells Regulate Plasma Cholesterol Levels and Development of Atherosclerosis in Humanized Hypercholesterolemic Mice

Editorial, see p 2527

Anton Gisterå, MD, PhD
Maria L. Klement, PhD
Konstantinos A. Polyzos, MD
Reiner K.W. Mailer, PhD
Amanda Duhlin, PhD
Mikael C.I. Karlsson, PhD
Daniel F.J. Ketelhuth, PhD
Göran K. Hansson, MD, PhD

BACKGROUND: Atherosclerotic cardiovascular disease is a chronic inflammatory process initiated when cholesterol-carrying low-density lipoprotein (LDL) is retained in the arterial wall. $CD4^+$ T cells, some of which recognize peptide components of LDL as antigen, are recruited to the forming lesion, resulting in T-cell activation. Although these T cells are thought to be proatherogenic, LDL immunization reduces disease in experimental animals. These seemingly contradictory findings have hampered the development of immune-based cardiovascular therapy. The present study was designed to clarify how activation of LDL-reactive T cells impacts on metabolism and vascular pathobiology.

METHODS: We have developed a T-cell receptor–transgenic mouse model to characterize the effects of immune reactions against LDL. Through adoptive cell transfers and cross-breeding to hypercholesterolemic mice expressing the antigenic human LDL protein apolipoprotein B-100, we evaluate the effects on atherosclerosis.

RESULTS: A subpopulation of LDL-reactive T cells survived clonal selection in the thymus, developed into T follicular helper cells in lymphoid tissues on antigen recognition, and promoted B-cell activation. This led to production of anti-LDL immunoglobulin G antibodies that enhanced LDL clearance through immune complex formation. Furthermore, the cellular immune response to LDL was associated with increased cholesterol excretion in feces and with reduced vascular inflammation.

CONCLUSIONS: These data show that anti-LDL immunoreactivity evokes 3 atheroprotective mechanisms: antibody-dependent LDL clearance, increased cholesterol excretion, and reduced vascular inflammation.

Key Words: apolipoprotein B-100 ■ atherosclerosis ■ hypercholesterolemia ■ T-lymphocytes ■ vaccination

Sources of Funding, see page 2524

https://www.ahajournals.org/journal/circ

ORIGINAL RESEARCH ARTICLE

Clinical Perspective

What Is New?

- Immune responses toward low-density lipoprotein (LDL) are important for atherosclerosis development, but a lack of specific experimental models has limited mechanistic understanding and translation of findings into clinical therapies.
- We developed T-cell receptor transgenic mice to study LDL autoimmunity in a humanized hypercholesterolemic mouse model of atherosclerosis.
- A strong T-cell–dependent B-cell response was induced by LDL, leading to production of anti-LDL immunoglobulin G (IgG) antibodies that enhanced LDL clearance and ameliorated atherosclerosis.

What Are the Clinical Implications?

- This study sheds light on the pathophysiological role of LDL-reactive T cells and anti-LDL IgG antibodies, both of which are known to be present in patients with atherosclerotic cardiovascular disease.
- We show that targeting LDL-reactive T cells can enhance atheroprotective immunity and that vaccination against LDL components may be an attractive way to prevent atherosclerosis.

Atherosclerotic cardiovascular disease is the main cause of death in the world today.[1] It is a chronic inflammatory process initiated when cholesterol-carrying low-density lipoprotein (LDL) particles are retained in the arterial wall.[2,3] LDL retention elicits a local inflammation with influx of monocytes that differentiate into macrophages, accumulate intracellular cholesterol, and produce inflammatory mediators.[4,5] In parallel with macrophages, T cells are also recruited to the forming lesion.[6,7] Many of them are CD4$^+$ cells that recognize LDL as an antigen, resulting in T-cell activation.[8,9] T cells accumulating in atherosclerotic lesions are largely of the proinflammatory T-helper (Th)1 subtype and produce inflammatory cytokines such as interferon γ and tumor necrosis factor,[8,10] which can activate other cells to secrete additional mediators, including interleukins (ILs), chemokines, and eicosanoids. Local production of inflammatory mediators in the atherosclerotic artery wall eventually leads to activation of acute phase responses and elevated levels of inflammatory markers such as IL-6 and C-reactive protein in the systemic circulation. Ongoing inflammatory and hemodynamic assault on the atherosclerotic lesion may ultimately cause a local dysfunction or breakdown of endothelial integrity. This, in turn, can trigger thrombus formation, local ischemia, and infarction of the end organ, as is the case in myocardial infarction and ischemic stroke.[2] This scenario can be prevented by anti-inflammatory therapy, as recently shown in a large secondary prevention clinical trial.[11]

The development of disease models in gene-targeted mice has permitted a dissection of the role of immunity and inflammation in atherosclerosis. By targeting key genes in cholesterol metabolism, it was possible to make mice severely hypercholesterolemic. This leads to the development of atherosclerosis in this species, although it is normally resistant to this disease.

Th1 cells and their signature cytokine, interferon γ, were found to exert proatherogenic effects in hypercholesterolemic, gene-targeted mice.[6,12,13] Such effects were also seen when CD4$^+$ T cells were introduced into immunodeficient *Apoe*$^{-/-}$*xscid/scid* mice.[14,15] Manipulation of regulatory T (Treg) cells revealed an atheroprotective role of this subset,[16–18] whereas Th17 cells may promote collagen formation and plaque stabilization.[19] All these studies involve genetic perturbation that affects global differentiation of T cells, and the impact of antigen-specific T-cell responses has remained unclear.

Immunization with LDL can elicit an atheroprotective response that inhibits lesion development.[20–22] This is the case irrespective of whether antigen is administered through the parenteral or mucosal route.[23] The atheroprotective effect appears to involve T cells because it is associated with the formation of high-titer immunoglobulin G (IgG)–anti-LDL.[22] It has been ascribed to the generation of immunosuppressive Tregs producing anti-inflammatory cytokines or to the formation of anti-LDL antibodies.[7]

During atherogenesis, periarterial and systemic B-cell responses also occur, with production of antibodies to epitopes on native and oxidized LDL particles.[24] Both pro- and antiatherosclerotic effects have been linked to B cells.[25–28] Thus, splenectomy increases disease in hypercholesterolemic mice, whereas transfer of spleen B cells reduces it.[25] Similarly, enhanced production of antibodies to epitopes on oxidized LDL particles attenuates disease development.[29] Paradoxically, administration of anti-CD20 antibodies also ameliorates it.[28]

Limited insights into the nature of the disease-associated immune response to LDL have made our understanding of the atherosclerotic process incomplete and hampered the possibilities to develop immunoprotective prevention and therapy. In other chronic inflammatory diseases, such as rheumatoid arthritis and multiple sclerosis, transgenic (tg) models, in which a large proportion of T cells recognize the purported autoantigens, have turned out to be useful for studies of pathogenetic mechanisms and therapeutic principles.[30,31] We therefore constructed a tg mouse model in which the majority of CD4$^+$ T cells recognize human LDL and determined its effects on LDL turnover and atherosclerosis.

METHODS

Mouse Strains

Three different T-cell receptors (TCRs) were cloned from hybridomas described previously.[9] The constructs were inserted into a hCD2-VA expression vector containing the promoter and locus control region of the human *CD2* gene.[32] The TCR α and β constructs were microinjected into C57BL/6J embryos at the Karolinska Center for Transgene Technologies, yielding a coisogenic C57BL/6J offspring that was screened for transgene expression by polymerase chain reaction. The 3 strains were named *BT1* (apoB-reactive T-cell strain 1) (TRAV12, TRBV31), *BT2* (TRAV4, TRBV31), and *BT3* (TRAV14, TRBV31). In subsequent experiments, C57BL/6J mice (*B6*) were used as controls. For LDL injections, the *BT* strains were crossed with a *Nur77-GFP* reporter mouse (C57BL/6-Tg(Nr4a1-EGFP/cre)820Khog/J, stock 016617; Jackson Laboratory). For cell transfers and crosses, we used *Human APOB100-tg Ldlr*^{tm1Her} (*HuBL*) mice backcrossed to C57BL/6J for 10 generations.[3] These mice carry the full-length human *APOB100* gene, in which codon 2153 has been converted from glutamine to leucine to prevent the formation of ApoB48 (apolipoprotein), thus generating only ApoB100. Mice were fed a Western diet (R638, Lantmännen) for 10 weeks.[9] All experiments were performed according to institutional guidelines and were approved by the Stockholm Regional Board for Animal Ethics.

Mouse Experiments

To measure T-cell activation in vivo, 10-week-old mice were injected with 100 µg LDL intraperitoneally. Sixteen hours later, spleens were harvested and T cells analyzed by flow cytometry. For adoptive T-cell transfer, 10-week-old male donors were euthanized and spleen and lymph nodes harvested. Single-cell suspensions were prepared and untouched CD4$^+$ cells isolated by negative selection with antibodies to CD8, CD11b, CD16/32, CD45R, and Ter-119 (Dynabeads untouched mouse CD4 cells kit, Invitrogen). Cells were labeled with CellTraceViolet (Invitrogen) or directly resuspended in phosphate-buffered saline (PBS) for intravenous injection of 3×10^6 cells in the tail vein. For cell trace experiments, recipients were euthanized 1 to 4 days after cell transfer. In other experiments, the recipients received the first injection at 10 weeks of age and a second injection at 15 weeks of age. They were euthanized at 20 weeks of age, after 10 weeks on a Western diet. All male *HuBL* progeny from the in-house breeding colony was included in the study and randomly assigned to receive B6, BT1, BT2, or BT3 cell transfer depending on available donors. The included mice were given a serial number to blind the following analyses. Two mice were excluded from the study, 1 died before the first injection, and the second died 25 days after the first BT2 cell injection. The study was closed when the number reached a predetermined power to detect a 10 percentage points difference in lesion size (aortic arches from untreated male *HuBL* mice were used for the power calculation; α=0.05, β=0.2). *BT1xHuBL* and *BT3xHuBL* mice were developed through crossbreeding. Hemizygous *BT1xHuBL* mice (homozygous for human *APOB100* and *Ldlr*^{tm1Her}) were then bred to *HuBL* mice to generate a *BT1*$^+$*xHuBL* study group and *BT1*$^-$*xHuBL* littermate controls (*HuBL*). Ten-week-old male mice were either fed a Western diet for 10 weeks or euthanized for baseline analyses.

For the vaccination study, 25-week-old male *HuBL* mice received subcutaneous immunizations with ApoB100 emulsified in complete Freund's adjuvant. The immune response was boosted 4 weeks later with ApoB100 emulsified in incomplete Freund's adjuvant. All mice received 100 µg protein. Control mice were immunized with PBS and adjuvant following the same protocol. All mice were euthanized 10 weeks after the first immunization.

Flow Cytometry Analysis

Flow cytometry was performed on leukocytes isolated as single-cell suspensions from spleen, thymus, or lymph nodes. Fixable Aqua Live/Dead staining was used according to the manufacturer's protocol (Invitrogen). After Fc-block (anti-CD16/32, BD Biosciences), fluorophore-labeled primary IgG antibodies were used for extracellular staining. Streptavidin Dylight 649 (Vector) was used for biotinylated primary antibodies. Intracellular staining was performed using the antimouse/rat Foxp3 staining set (eBioscience). All antibodies are listed in the Methods in the online-only Data Supplement. Samples were acquired on a CyAn ADP flow cytometer (Beckman Coulter), and data were analyzed using FlowJo software (Tree Star).

Tissue Processing, Immunohistochemistry, and Lesion Analysis

Blood from euthanized mice was collected by cardiac puncture and the vasculature perfused with sterile ribonuclease-free PBS. The aortic arch was fixed in PBS-buffered 4% formaldehyde solution for later pinning and staining with Sudan IV (Sigma-Aldrich). The rest of the aorta, para-aortic lymph nodes, and liver lobe were dissected and snap-frozen for later RNA isolation. The heart, spleen, liver, kidney, and duodenum were dissected and preserved in optimal cutting temperature compound for immunohistochemistry. Lesion analysis was performed as previously described.[9] Briefly, hearts were serially sectioned on a cryostat, starting from the proximal part of the aortic root, and stained with hematoxylin and Oil Red O. Kidney and liver sections were stained in the same way. Lesion size was determined on 8 sections, collected at every 100 µm of the aortic root. For each section, images were captured in a Leica photomicroscope, and the surface areas of the lesions and the entire vessel were measured using Image J software (National Institutes of Health). For fluorescent staining of spleen, liver, kidney, and duodenum sections, peanut agglutinin (Vector), Nile Red (Sigma-Aldrich), or antibodies listed in Methods in the online-only Data Supplement were used. Nuclei were stained with DAPI (4',6-diamidino-2-phenylindole; Sigma-Aldrich). Fluorescent micrographs were acquired with an SP2 Acusto-Optical Beam Splitter confocal laser-scanning microscope (Leica).

Blood and Plasma Analyses

Blood was collected by cardiac puncture or through tail vein bleeding in EDTA-coated tubes. Whole blood and splenocyte single-cell suspensions were analyzed on a Vet abc hemocounter (Scil). Plasma cholesterol and triglycerides were analyzed using enzymatic colorimetric kits (Randox) according to

the manufacturer's protocol. For lipoprotein profiling, plasma was fractionated using a Superose 6 10/300 GL column (GE Healthcare) coupled to a Prominence UFLC system (Shimadzu) and equilibrated with Tris-buffered saline, pH 7.4. Fractions of 200 µL were collected using a Foxy Jr fraction collector (Teldyne Isco) for subsequent detection of cholesterol and triglycerides with the previously mentioned enzymatic kits.

Titers of specific antibodies to LDL, oxidized (ox)LDL, and ApoB100 were measured with ELISA. In brief, 50 µl of the different antigens (10 µg/mL) were added to 96-well ELISA plates and incubated overnight at 4°C. Coated plates were washed with PBS and blocked with 1% gelatin (Invitrogen) in PBS for 1 hour at room temperature. Next, plates were washed and incubated for 2 additional hours with plasma from individual animals and diluted in Tris-buffered saline with 0.1% gelatin. After washing, total IgM (Immunkemi), IgG (Vector), IgG1 (Southern Biotech), and IgG2c (BD Biosciences) levels were revealed by using biotinylated antimouse antibodies and horseradish peroxidase (HRP)-streptavidin. The plates were washed, colorimetric reactions developed using tetramethylbenzidine (BD Biosciences), and absorbance measured on a microplate reader (Molecular Devices). For immune complex analysis, ELISA plates were coated with anti-ApoB100 antibodies and then incubated with mouse plasma to allow binding of LDL particles in the samples. After washing, any IgM and IgG bound to the LDL particles was detected by using biotinylated antibodies, HRP-streptavidin, and tetramethylbenzidine as described earlier.

For the competition ELISA, IgG antibodies (10 µg/mL) obtained from the plasma of *HuBL* and *BT3xHuBL* mice were preincubated with increasing amounts of native LDL, oxLDL, and ApoB overnight at 4°C in glass tubes. The mixtures were then used in ELISA assays detecting IgG antibodies to LDL and oxLDL as described previously.

Statistical Analysis

Data were analyzed using Prism version 5.03 for Windows (GraphPad). The Student's *t* test, 1-way ANOVA with Dunnett's multiple comparison test, or 2-way ANOVA with Bonferroni's posttest was used for comparisons when the Shapiro-Wilk test indicated normality. The Mann-Whitney or Kruskal-Wallis test with Dunn's multiple comparison test was used when Gaussian distribution could not be assumed. The Pearson correlation coefficient was used to assess correlations. Differences between groups were considered significant at *P* values <0.05 (*$P \le 0.05$, **$P \le 0.01$, ***$P \le 0.001$). All experiments were repeated at least twice. The data, analytic methods, and study materials will be made available to other researchers for purposes of reproducing the results or replicating the procedure (available at the authors' laboratories).

RESULTS

LDL-Reactive TCR-tg Mice

A panel of CD4+ T-cell hybridomas was established from mice immunized with human LDL particles. These cells recognized epitopes in the ApoB100 protein of LDL.[9] TCR cDNA from these cells was cloned under the *CD2* promoter and used for the production of tg mice. Three tg strains with strong anti-LDL reactivity, termed *BT1*, *BT2*, and *BT3*, were used for experiments (Figure 1A and Figure IA through IC in the online-only Data Supplement). They all expressed tg TCR with β-chain TRBV31 together with α-chain TRAV12, TRAV4, or TRAV14, respectively. TRBV31 was found on >90% of all CD4+ T cells in the tg strains but only on 8% of CD4+ T cells in wild-type mice (Figure 1B and Figure ID and IE in the online-only Data Supplement). Nearly all these cells were naïve in the tg mice (Figure 1B and Figure IF through IH in the online-only Data Supplement), but exposure to human native LDL in vitro evoked a strong T-cell response (Figure 1A and Figure IB in the online-

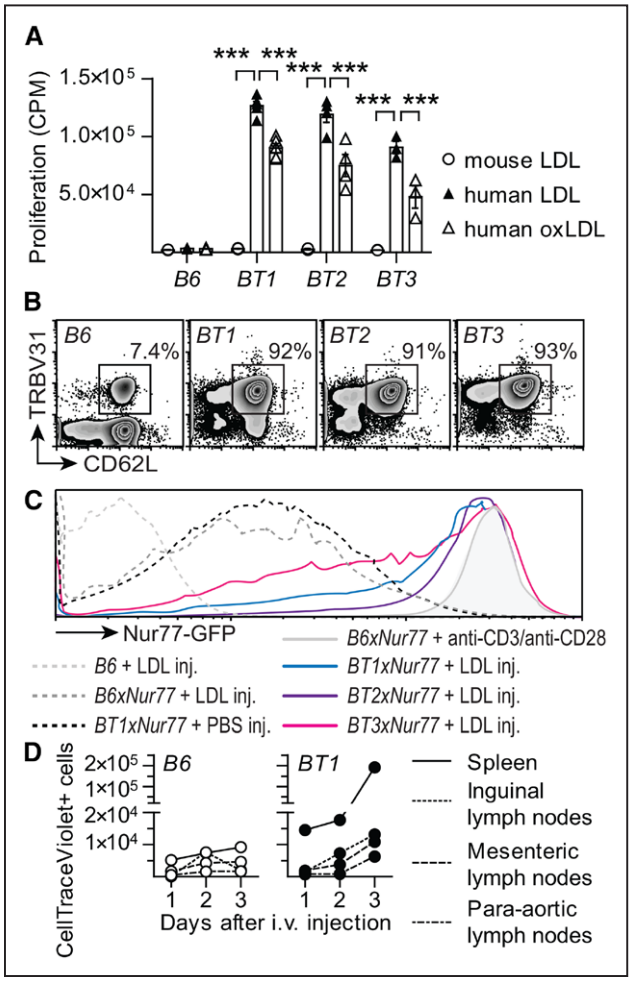

Figure 1. T-cell phenotype in *BT* transgenic mice.
A, Splenocytes incubated in triplicates with different stimuli for 60 hours in vitro. The mean proliferation is expressed as counts per minute (CPM) for unstimulated cells and cells stimulated with 10 µg/mL mouse LDL, human LDL, or oxidized human LDL (*B6* n=2–3, *BT1* n=3–4, *BT2* n=2–4, *BT3* n=2–4; 2-way ANOVA with Bonferroni's posttest, dots represent individual mice, bars show mean±SEM; ***$P \le 0.001$). **B**, Representative flow cytometry plots of expression of TRBV31 and CD62L in CD4+ T-helper cells. **C**, Flow cytometry histogram of Nur77-GFP expression in splenic TRBV31+CD3+CD4+ T-helper cells 16 hours after injection (inj) of 100 µg LDL intraperitoneally, showing 1 representative experiment of 3. **D**, CD4+ T-cell proliferation in *HuBL* mice. Proliferation of CD4+ T-helper cells labeled with CellTraceViolet transferred to *HuBL* recipients that express the antigen for BT1 cells. (*HuBL*/B6 n=3, *HuBL*/BT1 n=3; each dot represents a separate organ). See also Figures I and II in the online-only Data Supplement. LDL indicates low-density lipoprotein.

only Data Supplement). The proliferative response to oxLDL was less pronounced (Figure 1A and Figure IC in the online-only Data Supplement), in line with previous findings.[9]

T-Cell Activation by Injection of LDL

To characterize the response to LDL antigen in vivo, we crossed the tg *BT* strains with a reporter mouse expressing green fluorescent protein under *Nur77*, a promoter transcribed during T-cell activation.[33] Injection of human LDL led to vivid T-cell activation responses of the same magnitude as those achieved after polyclonal stimulation (Figure 1C and Figure II through IL in the online-only Data Supplement).

Injection of BT1 T Cells to *HuBL* Mice

T-cell activation in vivo was further studied by injecting BT1 T cells labeled with cell trace violet into *HuBL* mice (Figure IIA in the online-only Data Supplement). These mice carry the human LDL protein, ApoB100, as a transgene.[3] Therefore, they produce humanized LDL particles similar to those used as antigen for donor mouse immunization and TCR cloning. High plasma concentrations of humanized LDL particles are found in the *HuBL* cross that lacks the LDL receptor. After intravenous infusion, BT1 T cells were rapidly activated and underwent several rounds of proliferation in the *HuBL* hosts (Figure 1D and Figure IIB through IID in the online-only Data Supplement). Induction of Foxp3$^+$ T regulatory cells could not be observed (Figure IIE in the online-only Data Supplement). Most BT1 cells homed to the spleen, with significant populations also in para-aortic, inguinal, and mesenteric lymph nodes (Figure 1D and Figure IIC in the online-only Data Supplement). No signs of proliferation or homing were observed when wild-type C57BL/6J (B6) T cells were injected into *HuBL* mice (Figure 1D and Figure IIB and IIC in the online-only Data Supplement). BT2 cell injections led to similar rapid proliferative responses in *HuBL* mice, whereas no proliferation occurred in *Ldlr*$^{-/-}$ mice that lacked tg production of human LDL antigen (Figure IIF in the online-only Data Supplement). These data show that tg BT cells maintained their reactivity to human LDL and normal homing capacity after transfer into *HuBL* mice.

Injected BT T Cells Promote T- and B-Cell Activation

The long-term effects of a strong cellular immune response to LDL were studied in *HuBL* mice receiving BT cells twice over a 5-week period (Figure 2A and Table I in the online-only Data Supplement). BT cells remained detectable in the spleen 5 weeks after the last injection (Figure 2B). Spleens were enlarged, with an increased proportion of tg TRBV31$^+$ effector T cells and an expanded population of T follicular helper (Tfh) cells (Figure 2C and 2D and Figure IIIA through IIIJ in the online-only Data Supplement). This was accompanied by an expansion of the Th cell pool and an increased conversion of Th cells from naïve to effector/memory phenotype (Figure IIIC through IIIE in the online-only Data Supplement). In transcript analysis of aortas, elevated levels of Foxp3, the master regulator of Treg, and to a lesser extent Tbx21, encoding the Th1-transcription factor Tbet, were found in the *HuBL*/BT3 group (Table II in the online-only Data Supplement). This was accompanied by elevated mRNA levels of their signature cytokines, interferon γ and IL-10, but also the Tfh-related cytokine Il21 was found to be markedly increased (Table II in the online-only Data Supplement). In draining lymph nodes, the increase in Il21 mRNA was particularly striking (Table II in the online-only Data Supplement). In spleens, we also observed the formation of germinal centers, expansion of the plasma cell pool, and production of IgG antibodies to LDL (Figure 2E through 2H and Figure IIIK through IIIO in the online-only Data Supplement). These antibodies recognized native and oxidized forms of LDL as well as ApoB100 protein (Figure 2H and 2I and Figure IVA through IVF in the online-only Data Supplement). Anti-ApoB100 antibodies were of both IgG1 and IgG2c isotypes (Figure 2J and 2K and Figure IVG and IVH in the online-only Data Supplement). The concomitant induction of Tfh cells, formation of germinal centers, expansion of plasma cells, and increase in anti-LDL IgG demonstrates that T cells reactive to LDL protein provide help for B-cell activation, leading to anti-LDL antibody production.

Lower Plasma Cholesterol Levels in BT-Injected Mice

At 15 weeks of age, 5 weeks after the first injection, strikingly lower plasma cholesterol was seen in *HuBL* mice injected with BT1 or BT3 cells (Figure 3A and Table I in the online-only Data Supplement) because of reduced levels of LDL and the very-LDL/chylomicron remnant fraction (Figure 3B). The effects on plasma triglycerides were similar to those on cholesterol (Figure 3C and 3D). We speculated that the reduction in plasma lipids could be because of antibody-dependent elimination of lipoprotein particles from circulation. In support of this notion, LDL particles in mice injected with BT3 cells were found to be covered with antibodies, forming LDL-IgG immune complexes (Figure 3E and Figure IVI and IVJ in the online-only Data Supplement). Plasma from *HuBL*/BT3 chimeras enhanced fluorescein isothiocyanate (FITC)-oxLDL uptake into cultured macrophages, providing further support for this notion (Figure 3F and 3G).

ORIGINAL RESEARCH ARTICLE

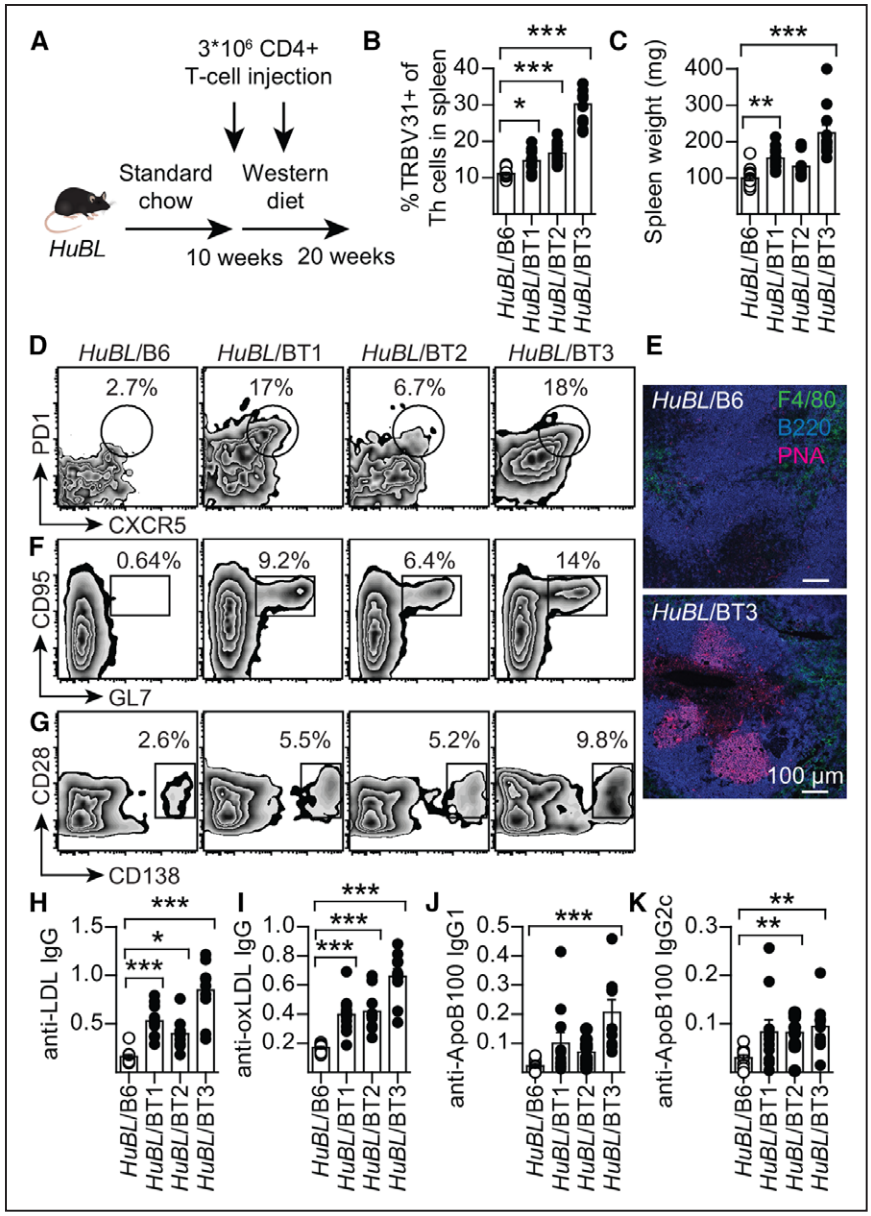

Figure 2. BT cells recognize LDL, develop into Tfh cells, and promote anti-LDL antibody production.
A, Experimental design of T-cell transfer experiment. **B**, Proportion TRBV31⁺ of T-helper cells in the spleen (*HuBL*/B6 n=14, *HuBL*/BT1 n=11, *HuBL*/BT2 n=10, *HuBL*/BT3 n=11; 1-way ANOVA with Dunnett's posttest). **C**, Spleen weight (Kruskal-Wallis test with Dunn's posttest). **D**, Flow cytometry plots of Tfh cell staining showing percentage of PD1⁺CXCR5⁺ Tfh cells in the CD44⁺CD62L⁻TRBV31⁺ Th population. **E**, Immunofluorescence micrographs showing B cells (B220⁺, blue), germinal centers (peanut agglutinin⁺ [PNA⁺], pink), and macrophages (F4/80⁺, green) in the spleen, with a 100-µm scale bar. **F**, Flow cytometry plots showing GL7⁺CD95⁺ germinal center B cells in the IgD^{low}CD19⁺B220⁺ B-cell population. **G**, Flow cytometry plots of CD138⁺ plasma cells in the B220^{low} lymphocyte population. **H**, Antinative LDL IgG antibodies (1:150 dilution, Kruskal-Wallis test with Dunn's posttest). **H**–**K**, Optical density at 450 nm is shown on *y* axis (*HuBL*/B6 n=12, *HuBL*/BT1 n=11, *HuBL*/BT2 n=10, *HuBL*/BT3 n=10). **I**, Anti-oxLDL IgG (1:150 dilution, 1-way ANOVA with Dunnett's posttest). **J** and **K**, Anti-ApoB100 IgG1 and IgG2c (1:15 dilution, Kruskal-Wallis test with Dunn's posttest). Dots represent individual mice, bars show mean±SEM; **P*≤0.05, ***P*≤0.01, ****P*≤0.001. See also Figures III and IV in the online-only Data Supplement. IgG indicates immunoglobulin G; and LDL, low-density lipoprotein.

Anti-LDL IgG Promotes LDL Clearance

To test whether anti-IgG antibodies promoted LDL clearance, FITC-labeled human LDL particles were mixed with anti-LDL IgG containing plasma from *HuBL*/BT3 mice or with plasma from control *HuBL*/B6 mice and injected into *HuBL* mice. FITC-LDL treated with *HuBL*/BT3 plasma displayed enhanced clearance compared with FITC-LDL treated with control plasma (Figure 3H). Lipid and IgG could be detected in kidney glomeruli of *HuBL*/BT3 animals, but creatinine levels remained normal (Figure IVK through IVM and Table I in the online-only Data Supplement). No increase of lipid-laden macrophages was observed in the spleen (Figure IVN in the online-only Data Supplement). Because the liver is a major site for clearance of IgG immune complexes,[34–36] we analyzed liver extracts but could not detect any accumulation of cholesterol (Figure IVO in the online-only Data Supplement). Therefore, further cholesterol clearance to feces is likely to occur if liver uptake of plasma lipoproteins is of importance for the cholesterol-lowering effect of the LDL immune response.

LDL-Reactive T Cells Protect From Atherosclerosis

Atherosclerotic lesion burden was reduced by 30% in the *HuBL*/BT3 and *HuBL*/BT1 animals, with a similar trend for *HuBL*/BT2 mice (Figure 3I and 3J). The different outcomes between the strains could be explained by different affinities and binding capacities to MHC class II-peptide complexes. A substantial downregulation of the BT2 TCR was observed in mediastinal lymph nodes (Figure 3K and 3L). Such a response is observed in high-affinity T-cell clones and can reduce their effector func-

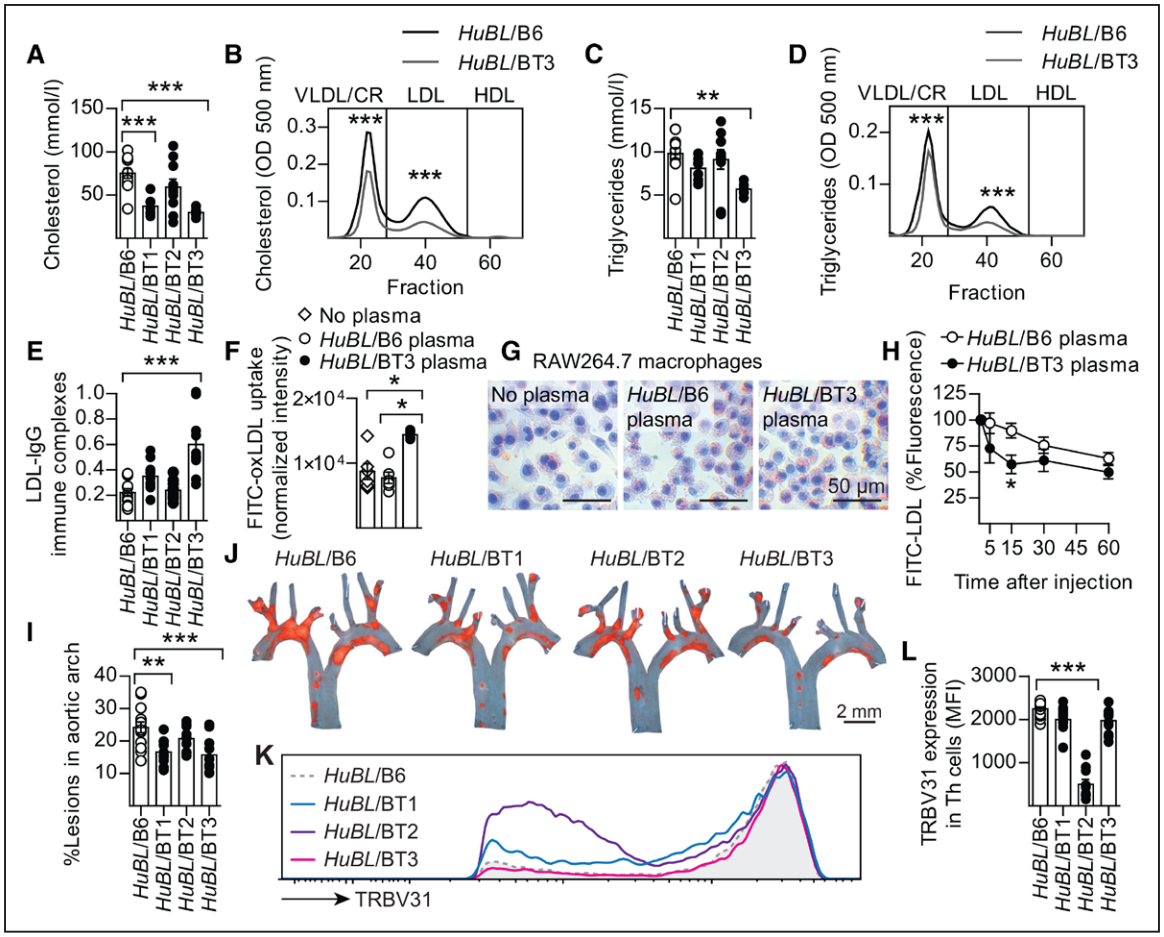

Figure 3. T-cell reactivity to LDL leads to reduced plasma lipids, formation of immune complexes, and reduced atherosclerosis.
A, Plasma cholesterol at 15 weeks of age after 5 weeks on Western diet (*HuBL*/B6 n=11, *HuBL*/BT1 n=7, *HuBL*/BT2 n=10, *HuBL*/BT3 n=7; 1-way ANOVA with Dunnett's posttest). **B**, Lipoprotein cholesterol profile (*HuBL*/B6 n=5, *HuBL*/BT3 n=5; 2-way ANOVA with Bonferroni's posttest, curve shows mean values). **C**, Plasma triglycerides (same statistics as in **A**). **D**, Lipoprotein triglyceride profile (same statistics as in **B**). **E**, Circulating immune complexes with LDL and anti-LDL IgG (optical density 450 nm, *HuBL*/B6 n=12, *HuBL*/BT1 n=11, *HuBL*/BT2 n=10, *HuBL*/BT3 n=10; 1:100 dilution, 1-way ANOVA with Dunnett's posttest). **F**, Uptake of oxLDL measured in RAW264.7 macrophages after 24 hours incubation with 25 µg/mL FITC-labeled oxLDL (no plasma n=6, *HuBL*/B6 plasma n=6, *HuBL*/BT3 plasma n=6; 1:100 plasma dilution, Kruskal-Wallis test with Dunn's posttest). **G**, Representative micrographs of hemtoxylin and Oil Red O–stained RAW264.7 macrophages after 24 hours incubation with 25 µg/mL oxLDL. **H**, Clearance of injected FITC-LDL particles pretreated with either *HuBL*/B6 or *HuBL*/BT3 plasma (*HuBL*/B6 plasma n=9, *HuBL*/BT3 plasma n=8; 2-way ANOVA with Bonferroni's posttest, graph shows mean±SEM). **I**, Atherosclerotic lesion burden in the aortic arch (*HuBL*/B6 n=14, *HuBL*/BT1 n=10, *HuBL*/BT2 n=10, *HuBL*/BT3 n=11; 1-way ANOVA with Dunnett's posttest). **J**, En face preparations of aortic arches with lipid-laden plaques stained with Sudan IV (orange color). **K**, Flow cytometry histogram of TRBV31 expression in $CD3^+CD4^+TRBV31^+$ lymphocytes to detect TCR downregulation in mediastinal lymph nodes. **L**, Mean fluorescence intensity (MFI) in T-helper cells (*HuBL*/B6 n=14, *HuBL*/BT1 n=12, *HuBL*/BT2 n=10, *HuBL*/BT3 n=12; 1-way ANOVA with Dunnett's posttest). Dots represent individual mice, bars show mean±SEM; $*P \le 0.05$, $**P \le 0.01$, $***P \le 0.001$. See also Figure IV in the online-only Data Supplement. CR indicates chylomicron remnants; HDL, high-density lipoprotein; and LDL, low-density lipoprotein.

tions.[37] Consequently, BT1 and BT3 cells may have lower affinities but more vigorous effector functions, including B-cell help and activation of cell-mediated immunity. Our findings are in line with this notion and also suggest that B-cell activation and production of antibodies capable of clearing the antigen contributed to the lipid-lowering effect of the anti-LDL immune response.

Thymic Selection of LDL-Reactive T Cells

BT1 mice were crossed with *HuBL* mice to study the development of the cellular immune response to LDL in a humanized model that produces the antigen from birth onwards (ie, a situation resembling that in humans). In both *HuBL* and *BT1xHuBL* mice, human *APOB100* was mainly expressed in the gut and liver, but mRNA could also be detected in the thymus, where it may aid negative selection against self-reactive T-cell clones (Figure 4A and 4B). A publically available dataset shows that Apob mRNA is expressed in medullary thymic epithelial cells (ie, the cells mainly responsible for negative thymic selection).[38] Most of the human ApoB100-reactive, $TRBV31^{bright}$ BT1 cells were eliminated in the thymus during early life, indicating that negative selection did take place against ApoB100 (Figure 4C through 4G and Figure VA in the online-only Data Supplement). However, ≈20% of $CD4^+$ T cells in the periphery were $TRBV31^{dim}$ in *BT1xHuBL* mice versus <1% in *B6xHuBL* animals (Figure 4H and Figure VB and VC and Table III in the online-only Data Supplement). TRBV31 could there-

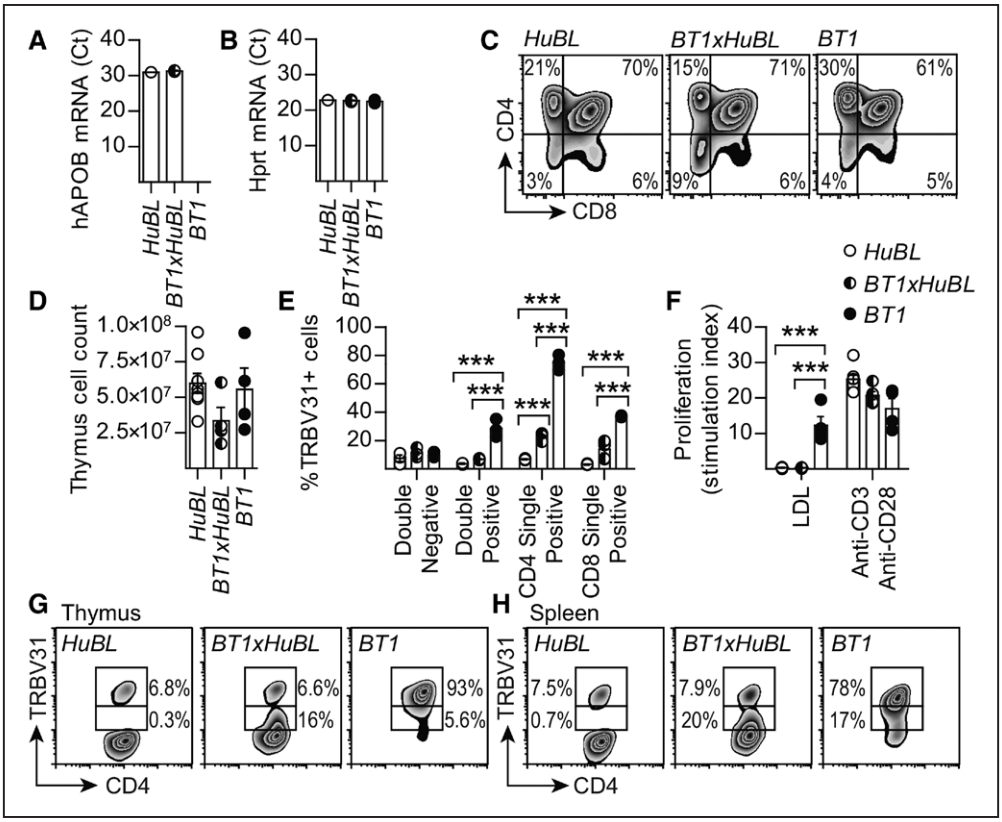

Figure 4. Survival of TRBV31^{dim} T cells in the *BT1xHuBL* cross.
A, Human APOB mRNA expression in the thymus, expression was not detected in the *BT1* strain lacking the human *APOB* transgene (Ct values, *HuBL* n=1, *BT1x-HuBL* n=3, *BT1* n=4). **B**, Hprt mRNA levels in the thymus, used as the housekeeping gene. **C**, Flow cytometry plots showing the expression of CD4 and CD8 in thymocytes. **D**, Number of cells in single-cell suspensions of thymus (*HuBL* n=8, *BT1xHuBL* n=4, *BT1* n=4). **E**, CD4$^-$CD8$^-$ double-negative, CD4$^+$CD8$^+$ double-positive, CD4 single-positive, and CD8 single-positive TRBV31$^+$ thymocytes (*HuBL* n=3, *BT1xHuBL* n=3, *BT1* n=3; 2-way ANOVA with Bonferroni's posttest). **F**, Proliferation of splenocytes from the indicated strains, stimulated with 10 μg/mL human LDL or anti-CD3/anti-CD28 (*HuBL* n=7, *BT1xHuBL* n=5, *BT1* n=4). Stimulation index is calculated as fold change of CPM over unstimulated cells. **G**, Flow cytometry plots showing TRBV31 expression by CD4 single-positive thymocytes in animals 10 weeks of age. **H**, Flow cytometry plots of TRBV31 expression in spleen CD4$^+$ T cells in animals 10 weeks of age. Dots represent individual mice; bars show mean±SEM; ***P≤0.001. See also Figure V in the online-only Data Supplement.

fore be used as a marker for tg cells. Detection of the tg α-chain was not possible with available antibodies, but its mRNA was overexpressed to a similar extent as that for the β-chain, and the levels of the 2 transcripts showed a strong positive correlation (Figure VD and VE and Table IV in the online-only Data Supplement). Among the TRBV31^{dim} cells, 10% to 15% were Tfh and Th1 effector cells (versus 2% to 6% in *B6xHuBL* mice), with a modest contribution of Foxp3$^+$ regulatory T cells (Figure 5A through 5C and Figure VF through VH and Table IV in the online-only Data Supplement). Transcript analysis of draining lymph nodes also showed a significant 36% reduction in IL-6 mRNA in the *BT1xHuBL* cross, implying reduced inflammatory activation (Table IV in the online-only Data Supplement).

Anti-LDL Immunity Protects Against Atherosclerosis

BT1xHuBL mice had increased plasma levels of anti-LDL IgG, including antibodies to oxLDL, native LDL, and ApoB100, mainly of the IgG1 isotype (Figure 5D through 5G and Figure VI through VP in the online-only Data Supplement). Similar to the cell transfer experiments, immune complex formation with LDL-[anti-LDL IgG] complexes was also detected in these animals (Figure 5H and Figure VQ and VR in the online-only Data Supplement). It was associated with significantly reduced plasma cholesterol, very-LDL, and LDL (Figure 5I and 5J and Figure VS through VU in the online-only Data Supplement). ApoB expression was not different in the liver or gut (Figure VIA and VIB and Table IV in the online-only Data Supplement), and cholesterol levels were decreased in liver extracts (Figure VIC and VID in the online-only Data Supplement).

Atherosclerotic lesions were substantially reduced, by ≈50%, in *BT1xHuBL* mice (Figure 5K through 5N and Figure VIE and VIF in the online-only Data Supplement). This outcome was accompanied by reduced expression of VCAM-1, a marker of vascular NF-κB activation, without any other significant effects on lesion composition (Figure VIG through VIM in the online-only Data Supplement). The disease burden was proportional to cholesterol levels (Figure VIN in the online-only Data

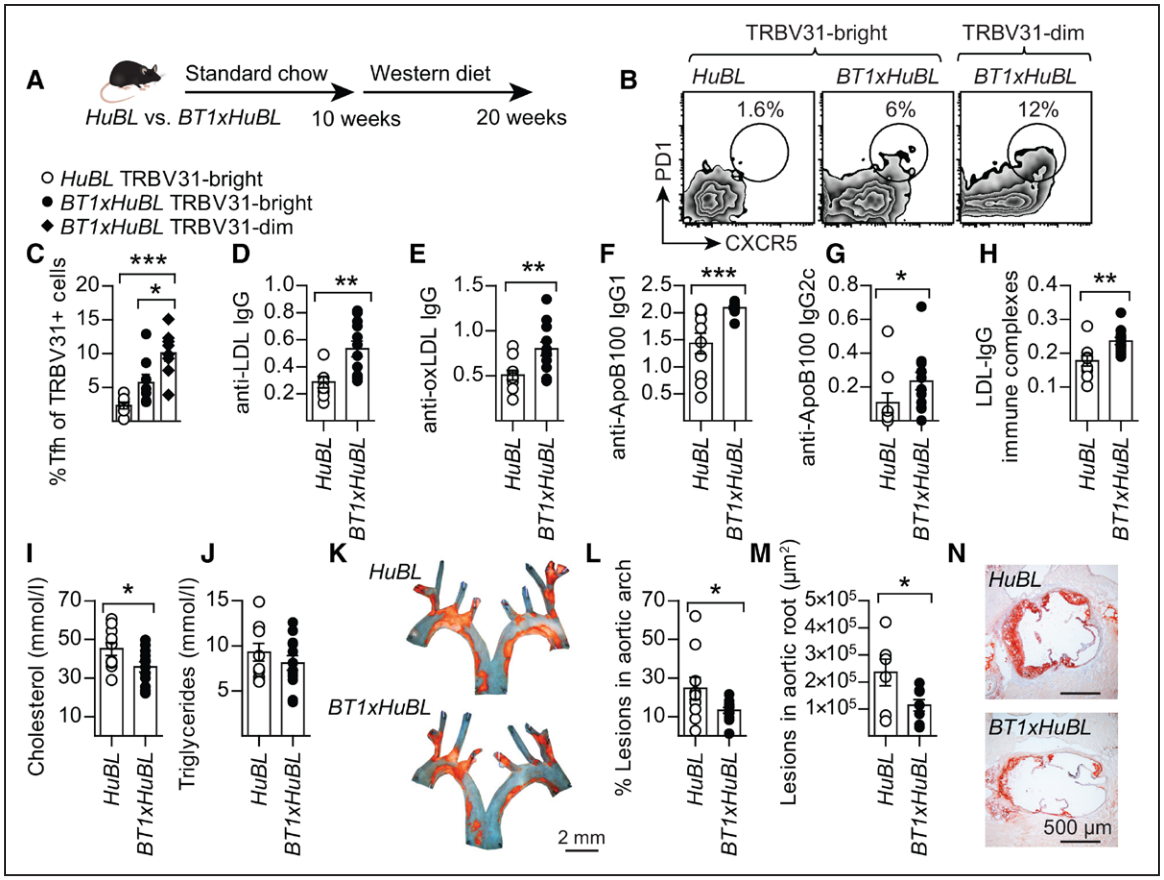

Figure 5. Induction of anti-LDL antibodies and protection against atherosclerosis in the *BT1xHuBL* cross.
A, Design of diet experiment with compound mutant mice. **B**, Representative flow cytometry plots of Tfh cell staining in the TRBV31^{bright} and TRBV31^{dim} populations. **C**, PD1^{+}CXCR5^{+} Tfh cells in the CD44^{+}CD62L^{-}TRBV31^{+} Th population (*HuBL* n=7, *BT1xHuBL* n=8; 1-way ANOVA with Bonferroni's posttest). **D**, Plasma anti-LDL IgG (*HuBL* n=9, *BT1xHuBL* n=12; 1:15 dilution, Student's *t* test). **D**–**H**, Optical density at 450 nm is shown on the *y* axis. **E**, Anti-oxLDL IgG (*HuBL* n=10, *BT1xHuBL* n=12; 1:15 dilution, Student's *t* test). **F** and **G**, Anti-ApoB100 IgG1 and IgG2c (*HuBL* n=10, *BT1xHuBL* n=12; 1:15 dilution, Mann-Whitney test). **H**, Circulating immune complexes with LDL and anti-LDL IgG (*HuBL* n=10, *BT1xHuBL* n=12; 1:100 dilution, Student's *t* test). **I** and **J**, Plasma cholesterol and triglycerides at 20 weeks of age (*HuBL* n=10, *BT1xHuBL* n=12; Student's *t* test). **K**, En face preparations of aortic arches with lipid-laden plaques stained with Sudan IV (orange). **L**, Atherosclerotic burden in aortic arch (*HuBL* n=10, *BT1xHuBL* n=12; Student's *t* test). **M**, Mean lesion area in the aortic root (*HuBL* n=7, *BT1xHuBL* n=8; Student's *t* test). **N**, Micrographs show Oil Red O staining of neutral lipids (red) in cross-sections of the aortic root. Dots represent individual mice, bars show mean±SEM; **P*≤0.05, ***P*≤0.01, ****P*≤0.001. See also Figures V and VI in the online-only Data Supplement. IgG indicates immunoglobulin G; and LDL, low-density lipoprotein.

Supplement) and showed a significant, negative correlation to immune complex concentration (Figure VIO in the online-only Data Supplement).

A similar atheroprotective effect was achieved when *HuBL* mice were immunized with ApoB preparations. This treatment also led to induction of IgG-anti-LDL antibodies, reduced plasma cholesterol, and reduced atherosclerosis (Figure 6A through 6D and Figure VIIA through VIIE in the online-only Data Supplement).

Clearance of Lipoproteins by a Humoral Response in *BT3xHuBL* Mice

Because BT3 cells induced the highest titers of anti-LDL antibodies, we crossed the *BT3* line with *HuBL* mice and investigated the phenotype of the offspring. The thymus of *BT3xHuBL* mice showed more pronounced signs of negative selection compared with *BT1xHuBL* mice (Figure VIIIA and VIIIB in the online-only Data Supplement). In the periphery, a reduction of Th cells was observed, but most of them were TRBV31^{+} effector/memory cells (Figure 7A and Figure VIIIC through VIIIG in the online-only Data Supplement). A significant proportion of the TRBV31^{dim} cells had differentiated into Tfh cells (Figure 7B). The enlarged spleen showed signs of ongoing inflammation and had increased germinal center B cells and plasma cells that produced high-titer anti-LDL IgG (Figure 7C and 7D and Figure VIIIH through VIIIO and Table V in the online-only Data Supplement). The B-cell response was further characterized by a competition assay in which purified IgG antibody binding to immobilized antigens was competed with soluble LDL, oxLDL, or ApoB100. This assay showed overlapping specificities between anti-LDL and anti-oxLDL antibodies (Figure 7E and 7F). LDL, oxLDL, and ApoB100 protein could all compete for binding. OxLDL was the most efficient competitor, indicating the presence of oxidation-specific epitopes. The pattern was similar to

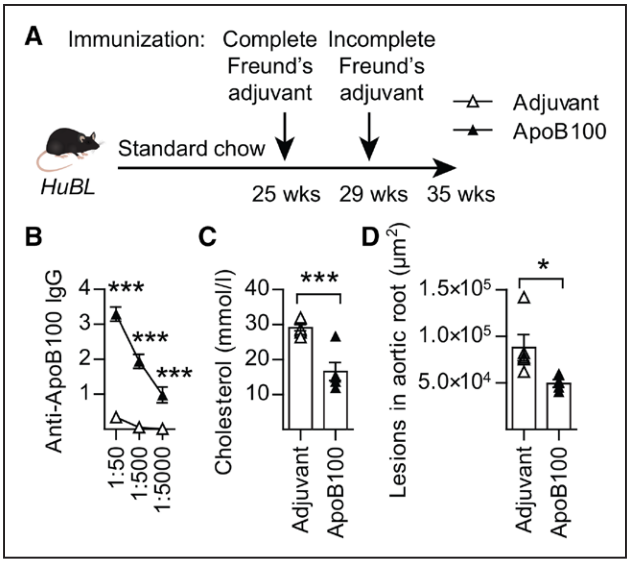

Figure 6. Lipid-lowering and atheroprotective ApoB100 vaccination. **A**, Experimental design of ApoB100 vaccination in *HuBL* mice. **B**, Anti-ApoB100 IgG titers, optical density at 450 nm on *y*-axis (*HuBL* mice; PBS-adjuvant n=6, ApoB100-adjuvant n=5; 2-way ANOVA with Bonferroni's multiple comparison test). **C**, Plasma cholesterol levels at 35 weeks of age (*HuBL* mice; PBS-adjuvant n=6, ApoB100-adjuvant n=5; Mann-Whitney test). **C** and **D**, Triangles represent individual mice and bars show mean±SEM. **D**, Mean atherosclerotic lesion area in the aortic root (*HuBL* mice; PBS-adjuvant n=5, ApoB100-adjuvant n=4; Mann-Whitney test). See also Figure VII in the online-only Data Supplemnt. Apo indicates apolipoprotein; and IgG, immunoglobulin G. *P≤0.05, ***P≤0.001.

HuBL IgG (Figure VIIIP and VIIIQ in the online-only Data Supplement).

In the circulation of *BT3xHuBL* mice, anti-LDL IgG formed immune complexes that were accompanied by lower plasma cholesterol and triglycerides and significant protection from atherosclerosis (Figure 7G through 7J and VIIIR and VIIIS in the online-only Data Supplement). Injection of IgG from these mice reduced plasma ApoB concentrations in recipients (Figure 7K and VIIIC in the online-only Data Supplement). These mice also displayed increased accumulation of lipids and IgG1 in the liver (Figure 7L through 7M and Figure VIIIT and VIIIU in the online-only Data Supplement). Further clearance of cholesterol to feces was also detected (Figure 7N). Lipoprotein production remained unaltered, as judged by ApoB expression in the liver and gut (Figure VIIIV through VIIIX in the online-only Data Supplement).

DISCUSSION

Our data provide insights into the mechanisms of atheroprotective immunity. They show that a subpopulation of LDL-reactive T cells survives clonal selection and is able to elicit adaptive immune reactions to LDL. Such reactions were mounted both to injected, autologous LDL and as a response to endogenously produced LDL in the humanized mouse. Therefore, LDL-reactive T cells can mount autoimmune reactions to lipoprotein particles.

When naïve LDL-reactive T cells were injected into mice producing human LDL, immune activation occurred in secondary lymphoid organs, including the spleen and draining lymph nodes. Although direct evidence is not available in mouse models, it is likely that recall activation of effector/memory T cells occurs in the diseased artery, as is the case in humans.[39]

The cellular immune response to LDL had important functional consequences, the net effect of which was a reduction of atherosclerosis. By providing B-cell help, it triggered formation of a set of anti-LDL antibodies that can enhance LDL clearance from circulation. Furthermore, the immune response to LDL was associated with increased cholesterol excretion and signs of reduced vascular inflammation. It is likely that all these effects synergized to inhibit disease development. These findings should be helpful in the development of immunotherapy against atherosclerotic cardiovascular disease.

The LDL-reactive T cells provided help for activation of LDL-reactive B cells. This process initiated germinal center reactions, with plasma cell formation and production of anti-LDL antibodies. Anti-LDL antibodies formed immune complexes with LDL that were detected in peripheral blood. Formation of immune complexes significantly increased clearance of LDL particles from the circulation, thus reducing plasma cholesterol levels, which is in line with findings made by Klimov et al[40] in the 1980s. Statistical analysis showed that LDL-[anti-LDL IgG] immune complexes, plasma cholesterol, and atherosclerotic lesion size were correlated, suggesting that these factors were dependent on each other. Our data point to the liver as the major site of elimination of lipoprotein-derived lipid; however, the detection of antibodies and lipid in the kidneys in 1 of the strains warrants further investigation.

Previous experiments to functionally assess the role of LDL-reactive T cells in atherogenesis have pointed to major roles for Th1 and Treg cells. We were not able to detect a decisive shift of these cell types, but the finding of reduced IL-6 expression in para-aortic lymph nodes of mice carrying strong LDL immunoreactivity suggests that local anti-inflammatory effects contributed to atheroprotection.

The most striking finding in our study was the induction of atheroprotective humoral immunity to LDL. The notion that LDL-reactive B cells mount atheroprotective immunity is in line with previous findings that B cells carry atheroprotective immunity,[25,26] atheroprotection is associated with the formation of IgG antibodies,[22] and disease is increased in mice lacking inhibitory and decreased in animals lacking activating Fc receptors.[41,42] Our current data extend these findings by demonstrating that humoral immunity to LDL is induced by Tfh effector cells that trigger B-cell activation, germinal center formation, and production

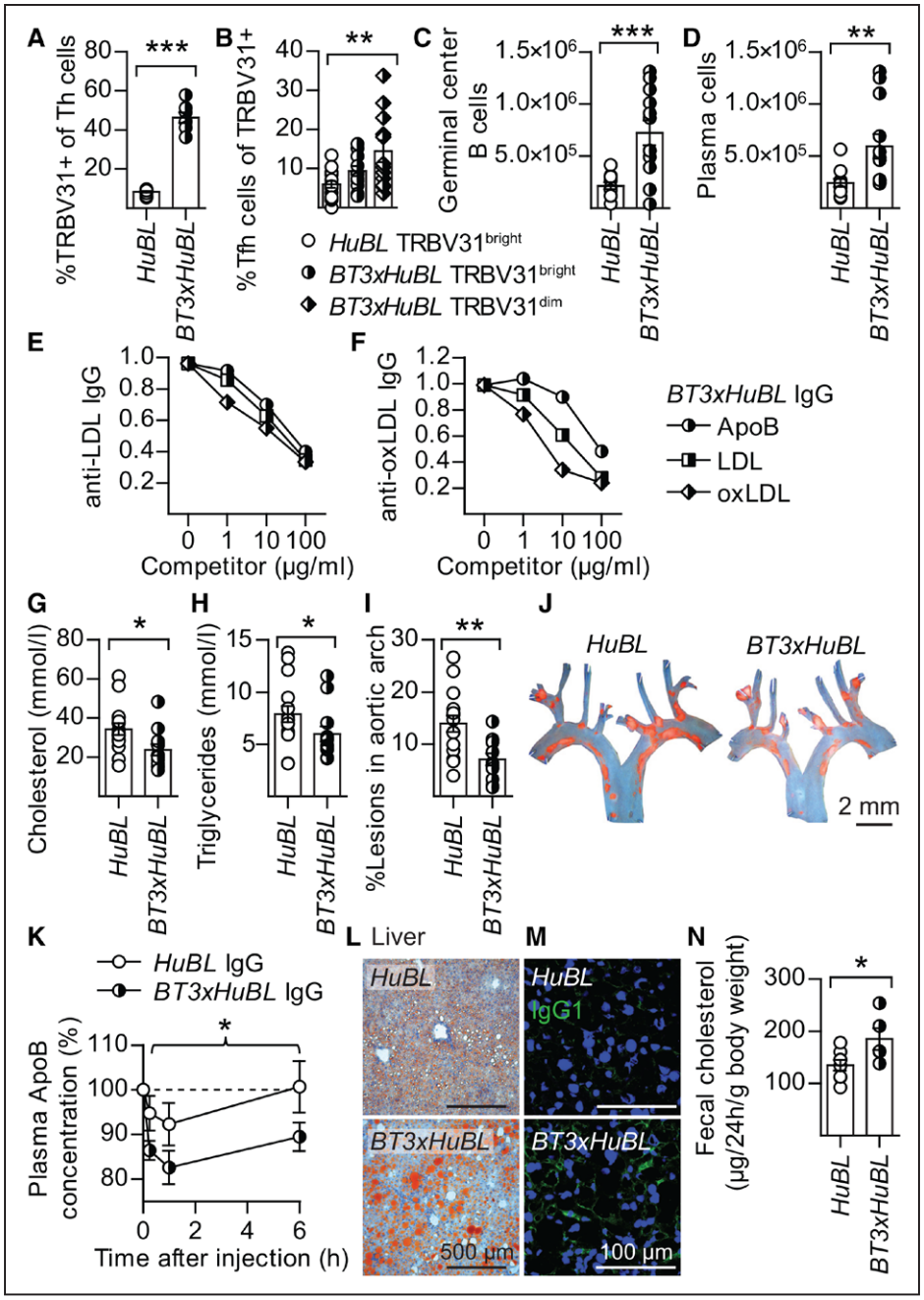

Figure 7. Lipid-lowering antibodies and reduced atherosclerosis in *BT3xHuBL* mice.
A, TRBV31⁺ T-helper cells in the spleen (*HuBL* n=16, *BT3xHuBL* n=7; Mann-Whitney test). **B**, PD1⁺CXCR5⁺ Tfh cells in the CD44⁺CD62L⁻TRBV31⁺ Th population (*HuBL* n=7, *BT3xHuBL* n=8; 1-way ANOVA with Bonferroni's posttest). **C**, GL7⁺CD95⁺IgD^{low} germinal center B cells (*HuBL* n=11, *BT3xHuBL* n=12; Student's *t* test). **D**, CD138⁺ plasma cells (*HuBL* n=11, *BT3xHuBL* n=12; Mann-Whitney test). **E**, Competition assay for evaluation of anti-LDL IgG specificity in total IgG isolated from *BT3xHuBL* mice (n=4; 2-way ANOVA with Bonferroni's posttest, significant competition by all 3 competitors). **F**, Competition assay for evaluation of anti-oxLDL IgG specificity in total IgG isolated from *BT3xHuBL* mice (n=4; 2-way ANOVA with Bonferroni's posttest, significant competition by all 3 competitors). **G**, Plasma cholesterol (*HuBL* n=16, *BT3xHuBL* n=12; Student's *t* test). **H**, Plasma triglycerides (*HuBL* n=16, *BT3xHuBL* n=12; Mann-Whitney test). **I**, Atherosclerotic burden in aortic arch (*HuBL* n=16, *BT3xHuBL* n=12; Student's *t* test). **J**, En face preparations of the aortic arch with lipid-laden plaques stained with Sudan IV (orange). **K**, ApoB measured in plasma at different time points after infusion of 200 µg IgG antibodies (*HuBL* mice; *HuBL* IgG n=4, *BT3xHuBL* IgG n=6; 2-way ANOVA, braces indicate significance level for treatment comparison, graph shows mean±SEM). **L**, Micrographs of Oil Red O–stained liver sections with a 500-µm scale bar. **M**, Immunofluorescence micrographs showing IgG1 (green) and cell nuclei (DAPI⁺, blue) in the liver, with a 100-µm scale bar. **N**, Cholesterol measured in lipid extracts from feces (*HuBL* n=8, *BT3xHuBL* n=5; Student's *t* test; each dot represents 1 cage). **A**–**D** and **G**–**I**, Dots represent individual mice; bars show mean±SEM. See also Figure VIII in the online-only Data Supplement. IgG indicates immunoglobulin G. **P*≤0.05, ***P*≤0.01, ****P*≤0.001.

of high-affinity antibodies to LDL. Furthermore, our data show that antibody-mediated clearance of LDL antigen contributed to the atheroprotective effect of LDL immunity.

The observed, incomplete tolerance to LDL and ApoB did not involve any substantial induction of natural Tregs but was because of clonal elimination in the thymus and peripheral anergy of cells escaping positive

selection. This finding does not rule out that peripheral tolerance mechanisms involving Treg may be important in atherosclerosis, and it should be kept in mind that the present experimental design involves transgenic TCR with high affinity to antigen. It is possible that T cells with lower affinity to antigen may play a significant role under normal conditions that do not involve genetically modified immune responses.

We have previously shown that the induction of antibodies that block the immunologic synapse of ApoB100-reactive T cells can reduce atherosclerosis.[9] It was, therefore, surprising that the net effect of a strong cellular immune response against the same antigen is atheroprotective. However, the 2 experiments are not directly comparable because synapse blockade likely inhibits all downstream effects of an immune response, whereas antigen activation of an antigen-specific T cell triggers a specific effector response that depends on the precise conditions at the time of activation, including the presence of specific metabolites, cytokines, and costimulatory factors. Furthermore, blockade of the immunologic synapse with an antibody to the pertinent TCR may exert immunomodulatory effects. Further studies are needed to elucidate the mechanisms leading to these results.

Our data clarify observations of antibody induction and plasma lipoprotein reduction in several experiments using immunization or anti-LDL IgG administration to control atherosclerosis.[27,29,43–46] The findings that T-cell reactions to LDL involve development of Tfh cells, germinal center formation, and antibody-dependent LDL clearance support and extend the recent report that formation of tertiary lymphoid structures protects against atherosclerosis.[47] These findings also shed light on the observation that disturbed T-cell migration leads to hypercholesterolemia, reduced anti-oxLDL antibodies, and increased atherosclerosis in mice[48] and that antibodies to oxLDL are inversely correlated with particle concentration in humans.[49] They are, however, seemingly at odds with studies showing proatherosclerotic effects of Tfh cells[50] and B2 cells.[28] In these reports, disease development was studied under conditions when global immunoregulatory networks were disrupted by mutations in the major histocompatibility complex and by administration of cytolytic antibodies, respectively. In contrast, our current data address the disease-associated autoimmunity to LDL and identify an atheroprotective mechanism elicited by the expansion of LDL-reactive T cells. Such T cells have been cloned from human atherosclerotic lesions[8] and are, therefore, active in clinical disease.

In humans, anti-LDL titers are generally low, and studies have shown weak or no associations between them and clinical cardiovascular events. It is, therefore, of interest to enhance immune responses in models to assess their pathophysiological consequences. It will also be important to develop and apply high-resolution imaging to measure lesion size in humans and determine its association with anti-LDL antibodies.

The models used in this study exaggerate hyperlipidemia as well as cellular immune reactivity and made it possible to study the effects of a strong immune response in a hyperlipidemic host within a reasonable time frame. They allowed us to analyze immune responses that may not be detectable in models with less profound immune reactivity toward LDL. It will now be important to follow these aspects of anti-LDL immunity in other models, expand the vaccination studies to characterize LDL-specific T-cell responses, and eventually translate the findings into human disease.

In conclusion, this study shows that T cells reactive to LDL survive clonal selection and can mount atheroprotective immune responses that involve humoral immunity, reduction of plasma cholesterol, and reduced lesion formation. By targeting LDL-reactive T cells, immunization with LDL protein can enhance such atheroprotective immunity. This may be an attractive way of inhibiting or preventing atherosclerotic cardiovascular disease.

ARTICLE INFORMATION

Received February 1, 2018; accepted June 27, 2018.

The online-only Data Supplement is available with this article at https://www.ahajournals.org/doi/suppl/10.1161/CIRCULATIONAHA.118.034076.

Correspondence

Göran K. Hansson, MD, PhD, Center for Molecular Medicine L8:03, Karolinska University Hospital, SE-17176 Stockholm, Sweden. Email Goran.Hansson@ki.se

Affiliations

Department of Medicine, Center for Molecular Medicine, Karolinska University Hospital (A.G., M.L.K., K.A.P., R.K.W.M., D.F.J.K., G.K.H.), and Department of Microbiology, Tumor and Cell Biology (A.D., M.C.I.K.), Karolinska Institutet, Stockholm, Sweden. Department of Immunotechnology, Lund University, Sweden (M.L.K.). Institute of Clinical Chemistry and Laboratory Medicine, University Medical Center Hamburg-Eppendorf, Germany (R.K.W.M.).

Acknowledgments

We thank I. Törnberg, L. Haglund, A. Olsson, R. Baumgartner, and A. Strodthoff for technical assistance.

Sources of Funding

This work was supported by project grant 06816 and Linnaeus support 349-2007-8703 from the Swedish Research Council and by grants from the Swedish Heart-Lung Foundation, the Swedish Foundation for Strategic Research (SSF), Vinnova Foundation, Stockholm County Council, King Gustav V and Queen Victoria Foundation, Prof Nanna Svartz foundation, the Novo Nordisk Foundation (NNF15CC0018346), and the European Union's Seventh Framework Program [FP7/2007–2013] under grant agreement Athero-Flux (No. 602222) and VIA (No. 603131). K.A.P. was supported by the Alexander S. Onassis foundation.

Disclosures

Drs Gisterå, Klement, Ketelhuth, and Hansson have filed patents on immunoprevention of atherosclerosis.

REFERENCES

1. Global, regional, and national age-sex specific mortality for 264 causes of death, 1980–2016: a systematic analysis for the Global Burden of Disease Study 2016. *Lancet*. 2017;390:1151–1210
2. Hansson GK. Inflammation, atherosclerosis, and coronary artery disease. *N Engl J Med*. 2005;352:1685–1695. doi: 10.1056/NEJMra043430
3. Skålén K, Gustafsson M, Rydberg EK, Hultén LM, Wiklund O, Innerarity TL, Borén J. Subendothelial retention of atherogenic lipoproteins in early atherosclerosis. *Nature*. 2002;417:750–754. doi: 10.1038/nature00804
4. Moore KJ, Tabas I. Macrophages in the pathogenesis of atherosclerosis. *Cell*. 2011;145:341–355. doi: 10.1016/j.cell.2011.04.005
5. Koenen RR, Weber C. Chemokines: established and novel targets in atherosclerosis. *EMBO Mol Med*. 2011;3:713–725. doi: 10.1002/emmm.201100183
6. Libby P, Lichtman AH, Hansson GK. Immune effector mechanisms implicated in atherosclerosis: from mice to humans. *Immunity*. 2013;38:1092–1104. doi: 10.1016/j.immuni.2013.06.009
7. Gisterå A, Hansson GK. The immunology of atherosclerosis. *Nat Rev Nephrol*. 2017;13:368–380. doi: 10.1038/nrneph.2017.51
8. Stemme S, Faber B, Holm J, Wiklund O, Witztum JL, Hansson GK. T lymphocytes from human atherosclerotic plaques recognize oxidized low density lipoprotein. *Proc Natl Acad Sci U S A*. 1995;92:3893–3897.
9. Hermansson A, Ketelhuth DF, Strodthoff D, Wurm M, Hansson EM, Nicoletti A, Paulsson-Berne G, Hansson GK. Inhibition of T cell response to native low-density lipoprotein reduces atherosclerosis. *J Exp Med*. 2010;207:1081–1093. doi: 10.1084/jem.20092243
10. Frostegård J, Ulfgren AK, Nyberg P, Hedin U, Swedenborg J, Andersson U, Hansson GK. Cytokine expression in advanced human atherosclerotic plaques: dominance of pro-inflammatory (Th1) and macrophage-stimulating cytokines. *Atherosclerosis*. 1999;145:33–43
11. Ridker PM, Everett BM, Thuren T, MacFadyen JG, Chang WH, Ballantyne C, Fonseca F, Nicolau J, Koenig W, Anker SD, Kastelein JJP, Cornel JH, Pais P, Pella D, Genest J, Cifkova R, Lorenzatti A, Forster T, Kobalava Z, Vida-Simiti L, Flather M, Shimokawa H, Ogawa H, Dellborg M, Rossi PRF, Troquay RPT, Libby P, Glynn RJ; CANTOS Trial Group. Antiinflammatory therapy with canakinumab for atherosclerotic disease. *N Engl J Med*. 2017;377:1119–1131. doi: 10.1056/NEJMoa1707914
12. Gupta S, Pablo AM, Jiang Xc, Wang N, Tall AR, Schindler C. IFN-gamma potentiates atherosclerosis in ApoE knock-out mice. *J Clin Invest*. 1997;99:2752–2761. doi: 10.1172/JCI119465
13. Buono C, Binder CJ, Stavrakis G, Witztum JL, Glimcher LH, Lichtman AH. T-bet deficiency reduces atherosclerosis and alters plaque antigen-specific immune responses. *Proc Natl Acad Sci U S A*. 2005;102:1596–1601. doi: 10.1073/pnas.0409015102
14. Zhou X, Nicoletti A, Elhage R, Hansson GK. Transfer of CD4(+) T cells aggravates atherosclerosis in immunodeficient apolipoprotein E knockout mice. *Circulation*. 2000;102:2919–2922.
15. Zhou X, Robertson AK, Hjerpe C, Hansson GK. Adoptive transfer of CD4+ T cells reactive to modified low-density lipoprotein aggravates atherosclerosis. *Arterioscler Thromb Vasc Biol*. 2006;26:864–870. doi: 10.1161/01.ATV.0000206122.61591.ff
16. Mallat Z, Besnard S, Duriez M, Deleuze V, Emmanuel F, Bureau MF, Soubrier F, Esposito B, Duez H, Fievet C, Staels B, Duverger N, Scherman D, Tedgui A. Protective role of interleukin-10 in atherosclerosis. *Circ Res*. 1999;85:e17–e24.
17. Robertson AK, Rudling M, Zhou X, Gorelik L, Flavell RA, Hansson GK. Disruption of TGF-beta signaling in T cells accelerates atherosclerosis. *J Clin Invest*. 2003;112:1342–1350. doi: 10.1172/JCI18607
18. Ait-Oufella H, Salomon BL, Potteaux S, Robertson AK, Gourdy P, Zoll J, Merval R, Esposito B, Cohen JL, Fisson S, Flavell RA, Hansson GK, Klatzmann D, Tedgui A, Mallat Z. Natural regulatory T cells control the development of atherosclerosis in mice. *Nat Med*. 2006;12:178–180. doi: 10.1038/nm1343
19. Gisterå A, Robertson AK, Andersson J, Ketelhuth DF, Ovchinnikova O, Nilsson SK, Lundberg AM, Li MO, Flavell RA, Hansson GK. Transforming growth factor-β signaling in T cells promotes stabilization of atherosclerotic plaques through an interleukin-17-dependent pathway. *Sci Transl Med*. 2013;5:196ra100. doi: 10.1126/scitranslmed.3006133
20. Palinski W, Miller E, Witztum JL. Immunization of low density lipoprotein (LDL) receptor-deficient rabbits with homologous malondialdehyde-modified LDL reduces atherogenesis. *Proc Natl Acad Sci U S A*. 1995;92:821–825.
21. Ameli S, Hultgårdh-Nilsson A, Regnström J, Calara F, Yano J, Cercek B, Shah PK, Nilsson J. Effect of immunization with homologous LDL and oxidized LDL on early atherosclerosis in hypercholesterolemic rabbits. *Arterioscler Thromb Vasc Biol*. 1996;16:1074–1079.
22. Zhou X, Caligiuri G, Hamsten A, Lefvert AK, Hansson GK. LDL immunization induces T-cell-dependent antibody formation and protection against atherosclerosis. *Arterioscler Thromb Vasc Biol*. 2001;21:108–114.
23. Klingenberg R, Lebens M, Hermansson A, Fredrikson GN, Strodthoff D, Rudling M, Ketelhuth DF, Gerdes N, Holmgren J, Nilsson J, Hansson GK. Intranasal immunization with an apolipoprotein B-100 fusion protein induces antigen-specific regulatory T cells and reduces atherosclerosis. *Arterioscler Thromb Vasc Biol*. 2010;30:946–952. doi: 10.1161/ATVBAHA.109.202671
24. Palinski W, Rosenfeld ME, Ylä-Herttuala S, Gurtner GC, Socher SS, Butler SW, Parthasarathy S, Carew TE, Steinberg D, Witztum JL. Low density lipoprotein undergoes oxidative modification in vivo. *Proc Natl Acad Sci U S A*. 1989;86:1372–1376.
25. Caligiuri G, Nicoletti A, Poirier B, Hansson GK. Protective immunity against atherosclerosis carried by B cells of hypercholesterolemic mice. *J Clin Invest*. 2002;109:745–753. doi: 10.1172/JCI7272
26. Major AS, Fazio S, Linton MF. B-lymphocyte deficiency increases atherosclerosis in LDL receptor-null mice. *Arterioscler Thromb Vasc Biol*. 2002;22:1892–1898.
27. Binder CJ, Hörkkö S, Dewan A, Chang MK, Kieu EP, Goodyear CS, Shaw PX, Palinski W, Witztum JL, Silverman GJ. Pneumococcal vaccination decreases atherosclerotic lesion formation: molecular mimicry between Streptococcus pneumoniae and oxidized LDL. *Nat Med*. 2003;9:736–743. doi: 10.1038/nm876
28. Ait-Oufella H, Herbin O, Bouaziz JD, Binder CJ, Uyttenhove C, Laurans L, Taleb S, Van Vré E, Esposito B, Vilar J, Sirvent J, Van Snick J, Tedgui A, Tedder TF, Mallat Z. B cell depletion reduces the development of atherosclerosis in mice. *J Exp Med*. 2010;207:1579–1587. doi: 10.1084/jem.20100155
29. Grasset EK, Duhlin A, Agardh HE, Ovchinnikova O, Hägglöf T, Forsell MN, Paulsson-Berne G, Hansson GK, Ketelhuth DF, Karlsson MC. Sterile inflammation in the spleen during atherosclerosis provides oxidation-specific epitopes that induce a protective B-cell response. *Proc Natl Acad Sci U S A*. 2015;112:E2030–E2038. doi: 10.1073/pnas.1421227112
30. Kouskoff V, Korganow AS, Duchatelle V, Degott C, Benoist C, Mathis D. Organ-specific disease provoked by systemic autoimmunity. *Cell*. 1996;87:811–822.
31. Goverman J, Woods A, Larson L, Weiner LP, Hood L, Zaller DM. Transgenic mice that express a myelin basic protein-specific T cell receptor develop spontaneous autoimmunity. *Cell*. 1993;72:551–560.
32. Zhumabekov T, Corbella P, Tolaini M, Kioussis D. Improved version of a human CD2 minigene based vector for T cell-specific expression in transgenic mice. *J Immunol Methods*. 1995;185:133–140.
33. Moran AE, Holzapfel KL, Xing Y, Cunningham NR, Maltzman JS, Punt J, Hogquist KA. T cell receptor signal strength in Treg and iNKT cell development demonstrated by a novel fluorescent reporter mouse. *J Exp Med*. 2011;208:1279–1289. doi: 10.1084/jem.20110308
34. Thornburg RW, Day JF, Baynes JW, Thorpe SR. Carbohydrate-mediated clearance of immune complexes from the circulation. A role for galactose residues in the hepatic uptake of IgG-antigen complexes. *J Biol Chem*. 1980;255:6820–6825.
35. Clarkson SB, Kimberly RP, Valinsky JE, Witmer MD, Bussel JB, Nachman RL, Unkeless JC. Blockade of clearance of immune complexes by an anti-Fc gamma receptor monoclonal antibody. *J Exp Med*. 1986;164:474–489.
36. Anderson CL, Ganesan LP, Robinson JM. The biology of the classical Fcγ receptors in non-hematopoietic cells. *Immunol Rev*. 2015;268:236–240. doi: 10.1111/imr.12335
37. Gallegos AM, Xiong H, Leiner IM, Sušac B, Glickman MS, Pamer EG, van Heijst JW. Control of T cell antigen reactivity via programmed TCR downregulation. *Nat Immunol*. 2016;17:379–386. doi: 10.1038/ni.3386
38. Ki S, Park D, Selden HJ, Seita J, Chung H, Kim J, Iyer VR, Ehrlich LIR. Global transcriptional profiling reveals distinct functions of thymic stromal subsets and age-related changes during thymic involution. *Cell Rep*. 2014;9:402–415. doi: 10.1016/j.celrep.2014.08.070
39. Stemme S, Holm J, Hansson GK. T lymphocytes in human atherosclerotic plaques are memory cells expressing CD45RO and the integrin VLA-1. *Arterioscler Thromb*. 1992;12:206–211.
40. Klimov AN, Denisenko AD, Popov AV, Nagornev VA, Pleskov VM, Vinogradov AG, Denisenko TV, Magracheva EYa, Kheifes GM, Kuznetzov AS.

Lipoprotein-antibody immune complexes: their catabolism and role in foam cell formation. *Atherosclerosis*. 1985;58:1–15.
41. Zhao M, Wigren M, Dunér P, Kolbus D, Olofsson KE, Björkbacka H, Nilsson J, Fredrikson GN. FcgammaRIIB inhibits the development of atherosclerosis in low-density lipoprotein receptor-deficient mice. *J Immunol*. 2010;184:2253–2260. doi: 10.4049/jimmunol.0902654
42. Hernández-Vargas P, Ortiz-Muñoz G, López-Franco O, Suzuki Y, Gallego-Delgado J, Sanjuán G, Lázaro A, López-Parra V, Ortega L, Egido J, Gómez-Guerrero C. Fcgamma receptor deficiency confers protection against atherosclerosis in apolipoprotein E knockout mice. *Circ Res*. 2006;99:1188–1196. doi: 10.1161/01.RES.0000250556.07796.6c
43. Freigang S, Hörkkö S, Miller E, Witztum JL, Palinski W. Immunization of LDL receptor-deficient mice with homologous malondialdehyde-modified and native LDL reduces progression of atherosclerosis by mechanisms other than induction of high titers of antibodies to oxidative neoepitopes. *Arterioscler Thromb Vasc Biol*. 1998;18:1972–1982.
44. Schiopu A, Bengtsson J, Söderberg I, Janciauskiene S, Lindgren S, Ares MP, Shah PK, Carlsson R, Nilsson J, Fredrikson GN. Recombinant human antibodies against aldehyde-modified apolipoprotein B-100 peptide sequences inhibit atherosclerosis. *Circulation*. 2004;110:2047–2052. doi: 10.1161/01.CIR.0000143162.56057.B5
45. Chyu KY, Zhao X, Reyes OS, Babbidge SM, Dimayuga PC, Yano J, Cercek B, Fredrikson GN, Nilsson J, Shah PK. Immunization using an Apo B-100 related epitope reduces atherosclerosis and plaque inflammation in hypercholesterolemic apo E (-/-) mice. *Biochem Biophys Res Commun*. 2005;338:1982–1989. doi: 10.1016/j.bbrc.2005.10.141
46. Habets KL, van Puijvelde GH, van Duivenvoorde LM, van Wanrooij EJ, de Vos P, Tervaert JW, van Berkel TJ, Toes RE, Kuiper J. Vaccination using oxidized low-density lipoprotein-pulsed dendritic cells reduces atherosclerosis in LDL receptor-deficient mice. *Cardiovasc Res*. 2010;85:622–630. doi: 10.1093/cvr/cvp338
47. Hu D, Mohanta SK, Yin C, Peng L, Ma Z, Srikakulapu P, Grassia G, MacRitchie N, Dever G, Gordon P, Burton FL, Ialenti A, Sabir SR, McInnes IB, Brewer JM, Garside P, Weber C, Lehmann T, Teupser D, Habenicht L, Beer M, Grabner R, Maffia P, Weih F, Habenicht AJ. Artery tertiary lymphoid organs control aorta immunity and protect against atherosclerosis via vascular smooth muscle cell lymphotoxin β receptors. *Immunity*. 2015;42:1100–1115. doi: 10.1016/j.immuni.2015.05.015
48. Klingenberg R, Nofer JR, Rudling M, Bea F, Blessing E, Preusch M, Grone HJ, Katus HA, Hansson GK, Dengler TJ. Sphingosine-1-phosphate analogue FTY720 causes lymphocyte redistribution and hypercholesterolemia in ApoE-deficient mice. *Arterioscler Thromb Vasc Biol*. 2007;27:2392–2399. doi: 10.1161/ATVBAHA.107.149476
49. Shoji T, Nishizawa Y, Fukumoto M, Shimamura K, Kimura J, Kanda H, Emoto M, Kawagishi T, Morii H. Inverse relationship between circulating oxidized low density lipoprotein (oxLDL) and anti-oxLDL antibody levels in healthy subjects. *Atherosclerosis*. 2000;148:171–177.
50. Clement M, Guedj K, Andreata F, Morvan M, Bey L, Khallou-Laschet J, Gaston AT, Delbosc S, Alsac JM, Bruneval P, Deschildre C, Le Borgne M, Castier Y, Kim HJ, Cantor H, Michel JB, Caligiuri G, Nicoletti A. Control of the T follicular helper-germinal center B-cell axis by $CD8^+$ regulatory T cells limits atherosclerosis and tertiary lymphoid organ development. *Circulation*. 2015;131:560–570. doi: 10.1161/CIRCULATIONAHA.114.010988